Highly nondegenerate four-wave mixing in semiconductor lasers due to spectral hole burning

Govind P. Agrawal
AT&T Bell Laboratories, Murray Hill, New Jersey 07974

(Received 26 February 1987; accepted for publication 4 June 1987)

Spectral hole burning in semiconductor lasers manifests as a nonlinear suppression of the mode gain by a few percent. In the presence of a probe wave, the same mechanism can lead to highly nondegenerate four-wave mixing (NDFWM) by creating the dynamic gain and index gratings at the beat frequency of the pump and probe waves. Since the grating efficiency is governed by the intraband relaxation time (typically <1 ps), significant NDFWM can occur even for a pump-probe detuning ~ 100 GHz. We present the results for the conjugate reflectivity and the probe transmittivity when an InGaAsP laser is used as a traveling-wave amplifier.

The nonlinear phenomenon of four-wave mixing has been widely studied[1] and, among other applications, constitutes a powerful tool for high-resolution spectroscopy. Recently it was demonstrated[2,3] that nondegenerate four-wave mixing (NDFWM) inside a semiconductor laser can be highly efficient at pump powers of only a few milliwatts. The physical mechanism behind NDFWM is Bragg scattering from the dynamic gain and index gratings created by the carrier-density modulation occurring at the beat frequency of the pump and probe waves.[4] The effectiveness of such gratings is governed by the spontaneous carrier lifetime (~ 2 ns). As a result, NDFWM ceases to occur when the pump-probe detuning exceeds a few gigahertz.

The objective of this letter is to show theoretically that an intraband mechanism in semiconductor lasers can lead to NDFWM even when the pump-probe detuning exceeds 100 GHz. The physical phenomenon behind highly NDFWM is spectral hole burning,[5,6] manifested as a nonlinear suppression of the mode gain in semiconductor lasers.[7-10] Since spectral hole burning is governed by the intraband relaxation processes occurring at a fast time scale (typically <1 ps), the dynamic grating remains an effective source of NDFWM for beat frequencies up to ~ 1 THz. The important point to note is that the gain and index gratings are not created by the carrier-density modulation but by the modulation of the occupation probability of carriers within a band (the Fermi factor of electrons in the case of the conduction band).

In the standard NDFWM geometry, two counterpropagating pump waves at the frequency ω_0 interact with a probe wave at ω_1 and generate a conjugate wave at the frequency $\omega_2 = 2\omega_0 - \omega_1$. The nonlinear interaction is governed by the scalar wave equation

$$\nabla^2 E - \frac{n^2}{c^2}\frac{\partial^2 E}{\partial t^2} = \frac{1}{\epsilon_0 c^2}\frac{\partial^2 P}{\partial t^2}, \tag{1}$$

where n is the refractive index, ϵ_0 is the vacuum permittivity, and c is the velocity of light in vacuum. The total electric field E is given by

$$E(x,y,z,t) = U(x,y)\sum_j E_j(z)\exp(-i\omega_j t), \tag{2}$$

where $j = 0$, 1, and 2 for pump, probe, and conjugate waves, respectively. The semiconductor laser structure is assumed to support only the fundamental waveguide mode with the distribution $U(x,y)$. This is generally the case for strongly index-guided lasers.[11] Similar to Eq. (2), the induced polarization P can also be written as

$$P(x,y,z,t) = U(x,y)\sum_j P_j(z)\exp(-i\omega_j t). \tag{3}$$

The induced polarization is calculated using the density-matrix formalism.[7,8] Each possible transition between the conduction- and valence-band states is modeled as a two-level system. The diagonal elements of the density matrix represent the occupation probabilities in the two bands and are affected by stimulated recombinations occurring at the pump and probe frequencies. Beating between the pump and probe fields results in a modulation of occupation probability (or the intraband carrier population) at the beat frequency $\Omega = \omega_1 - \omega_0$. This in turn creates the dynamic gain and index gratings which generate the conjugate wave at $\omega_2 = \omega_0 - \Omega$ through Bragg scattering. We follow the treatment of Kazarinov *et al.*[7] and make the same simplifying assumption: the probe and conjugate fields are less intense compared to the pump field so that third-order perturbation theory can be employed. The polarization components P_1 and P_2 for the probe and conjugate waves are then given by[7,10]

$$P_1 = \epsilon_0[\chi_L(\omega_1) + \chi_1(\Omega) + \chi_2(\Omega)]E_1 + \epsilon_0\chi_3(\Omega)E_2^*, \tag{4a}$$

$$P_2 = \epsilon_0[\chi_L(\omega_2) + \chi_1(-\Omega) + \chi_2(-\Omega)]E_2 + \epsilon_0\chi_3(-\Omega)E_1^*, \tag{4b}$$

where

$$\chi_L(\omega_j) = -\frac{(\beta_c + i)nc}{\omega_j}g(\omega_j) \quad (j = 1,2) \tag{5}$$

is the linear susceptibility, $g(\omega_j)$ is the mode gain, and β_c accounts for the carrier-induced reduction in the refractive index that always accompanies the gain in semiconductor lasers.[11]

The nonlinear contribution to the induced polarization is governed by χ_1, χ_2, and χ_3. In particular, χ_1 is due to a static change in the intraband population while χ_2 and χ_3

 0003-6951/87/310302-03$01.00

have their origin in the dynamic variation of the intraband population due to pump-probe beating. The explicit expressions of χ_1, χ_2, and χ_3 are[7,10]

$$\chi_1(\Omega) = \frac{inc}{\omega_0} \frac{g_s C(1-i\beta)}{(1-i\Omega T_2/2)} \frac{|E_0|^2}{I_s}, \tag{6}$$

$$\chi_2(\Omega) = \frac{inc}{\omega_0} \frac{g_s C(1-i\beta)}{(1-i\Omega T_2/2)(1-i\Omega T_1)} \frac{|E_0|^2}{I_s}, \tag{7}$$

$$\chi_3(\omega) = \frac{inc}{\omega_0} \frac{g_s C[1-i\beta(1-i\Omega T_2)]}{(1-i\Omega T_2)(1-i\Omega T_1)} \frac{E_0^2}{I_s}. \tag{8}$$

In Eqs. (6)–(8), T_1 is the intraband population relaxation time, T_2 is the polarization relaxation time, and $I_s = \hbar^2/(\mu^2 T_1 T_2)$ is the saturation intensity for a transition with the dipole moment μ. The saturated gain $g_s = g_0/(1+|E_0|^2/I_s)$, where g_0 is the small-signal gain. The parameter

$$\beta = \frac{1}{g_0 T_2}\left(\frac{dg}{d\omega}\right)_{\omega=\omega_0} \tag{9}$$

is related to the slope of the gain profile at the pump frequency ω_0 and g_0 is the gain at that frequency. The overlap factor

$$C = \langle |U(x,y)|^4 \rangle / \langle |U(x,y)|^2 \rangle \tag{10}$$

arises from the spatial structure of the waveguide mode; the angle brackets denote averaging over the waveguide cross section.

This completes the general formalism. For its application, one should distinguish whether the laser is operating below or above threshold. In the latter case, the pump wave is internally generated, and the gain g_0 in Eqs. (6)–(8) is clamped at its threshold value. The injection of a probe at a frequency shifted by Ω from the laser frequency leads to NDFWM. Although the case of above-threshold operation is of practical interest, the theoretical analysis is complicated as one has to consider the forward and backward waves together with the appropriate boundary conditions at the laser facets for pump, probe, and conjugate waves.[3]

To show the main qualitative features of NDFWM as simply as possible, we consider the case of below-threshold operation of the semiconductor laser. Furthermore, we assume that the laser operates as a traveling-wave amplifier with negligible facet reflectivities (by the use of an antireflection coating). In the collinear geometry, the pump, probe, and conjugate fields are then of the form

$$E_0 = \sqrt{I_s}\,[A_f \exp(ik_0 z) + A_b \exp(-ik_0 z)], \tag{11a}$$

$$E_1 = \sqrt{I_s} A_1 \exp(ik_1 z), \tag{11b}$$

$$E_2 = \sqrt{I_s} A_2 \exp(-ik_2 z), \tag{11c}$$

where $k_j = n\omega_j/c$. If we use Eqs. (2), (3), and (11) in Eq. (1) and make the paraxial approximation, we obtain

$$\sqrt{I_s}\frac{dA_j}{dz} = \pm \frac{i\omega_j}{2\epsilon_0 nc} P_j \exp(\mp ik_j z). \tag{12}$$

Using Eqs. (4) and (12) and keeping only the nearly phase-matched terms, we obtain the coupled wave equations for the conjugate and probe fields:

$$\frac{DA_1}{dz} = -\alpha_1 A_1 + i\kappa_1 A_2^* \exp(i\Delta k z), \tag{13a}$$

$$\frac{dA_2^*}{dz} = +\alpha_2^* A_2^* + i\kappa_2^* A_1 \exp(-i\Delta k z), \tag{13b}$$

where $\Delta k = k_2 - k_1 = -2n\Omega/c$ is the wave-number mismatch and

$$\alpha_1 = -\frac{g_s}{2}\left[1 - i\beta_c - \frac{\Omega^2}{\Delta\omega_g^2} + \frac{C(1-i\beta)(|A_f|^2+|A_b|^2)}{(1-i\Omega T_2/2)} \times\left(1+\frac{1}{1-i\Omega T_1}\right)\right], \tag{14}$$

$$\kappa_1 = \frac{i}{2}\frac{g_s C[1-i\beta(1-i\Omega T_2)]}{(1-i\Omega T_2)(1-i\Omega T_1)}(2A_f A_b). \tag{15}$$

The expressions for α_2 and κ_2 are obtained by changing Ω to $-\Omega$ in Eqs. (14) and (15). The gain rolloff is accounted for by $\Delta\omega_g$ in Eq. (14). We have neglected the interference term in $|E_0|^2$. This is reasonable since carrier diffusion reduces the effectiveness of spatial hole burning in semiconductor lasers. Both α_j and κ_j in Eqs. (13) are z dependent because A_f and A_b vary exponentially along the amplifier length. To simplify the analysis, we average them over the length L and use

$$\langle |A_f(z)|^2 + |A_b(z)|^2 \rangle = 2P_{\rm in}\left[(e^{g_s L}-1)/g_s L\right], \tag{16}$$

$$\langle A_f(z) A_b(z) \rangle = P_{\rm in} \exp(g_s L/2), \tag{17}$$

where $P_{\rm in} = |A_f(0)|^2 = |A_b(L)|^2$ is the incident pump intensity.

Owing to their linearity, Eqs. (13) are readily solved. The expressions for the phase-conjugate reflectivity R and the probe transmittivity T are[12,13]

$$R = \left|\frac{A_2^*(0)}{A_1(0)}\right|^2 = \left|\frac{\kappa_2 \sin(pL)}{p\cos(pL) + \alpha \sin(pL)}\right|^2, \tag{18}$$

$$T = \left|\frac{A_1(L)}{A_1(0)}\right|^2 = \left|\frac{p\exp(-\bar{\alpha}L)}{p\cos(pL) + \alpha\sin(pL)}\right|^2, \tag{19}$$

where L is the laser length and

$$p = (\kappa_1\kappa_2^* - \alpha^2)^{1/2}, \quad \alpha = \tfrac{1}{2}(\alpha_1 + \alpha_2^* + i\Delta k), \tag{20}$$

$$\bar{\alpha} = \tfrac{1}{2}(\alpha_1 - \alpha_2^* - i\Delta k). \tag{21}$$

To estimate R and T, we consider a 1.55-μm InGaAsP laser with typical parameter values $g_0 L = 6$, $C = 0.7$, $\beta = 0$, $\beta_c = 5$, $\Delta\omega_g \simeq T_2^{-1}$, $T_1 = 0.3$ ps, and $T_2 = 0.1$ ps. A gain of $g_0 L = 6$ can be achieved for a semiconductor-laser amplifier with facet reflectivities of $< 1\%$. The choice $\beta = 0$ is appropriate when the pump frequency coincides with the gain peak. It is important to account for the phase mismatch because of the nondegenerate nature of NDFWM. Note that $|\Delta k L| = 2|\Omega|\tau$, where τ is the transit time ($\tau \simeq 3$ ps for $L = 250\,\mu$m); we choose $\tau/T_1 = 10$. Figures 1 and 2 show the variation of R and T with the normalized pump-probe detuning ΩT_1 for three values of the incident pump power (assuming a saturation power of 100 mW). When $\Omega T_1 < 0.2$, the conjugate reflectivity R can exceed 100% for a few mW of pump powers; $\Omega T_1 = 0.2$ corresponds to a pump-probe detuning of about 100 GHz. In fact, NDFWM is limited by the transit time rather than the medium response time, in contrast to the case discussed in Ref. 4. Thus, significant NDFWM can occur even for larger pump-probe detunings if the transit time is shortened by reducing the amplifier length. The weak satellite peaks in the reflectivity spectra in Fig. 1 are also due to the phase mismatch.

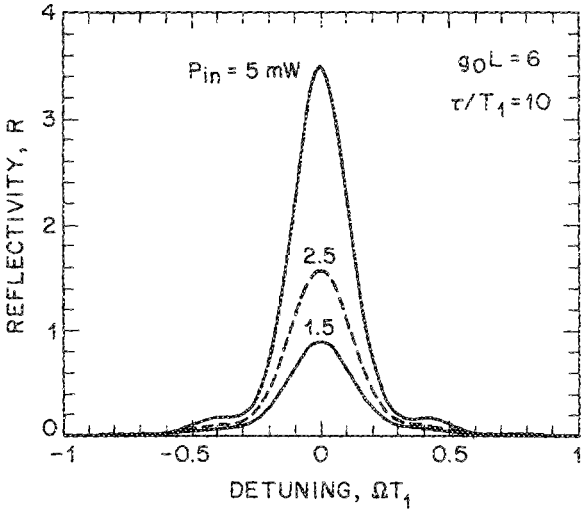

FIG. 1. Variation of the conjugate reflectivity R with the normalized pump-probe detuning ΩT_1 for three values of the incident pump intensity P_{in}.

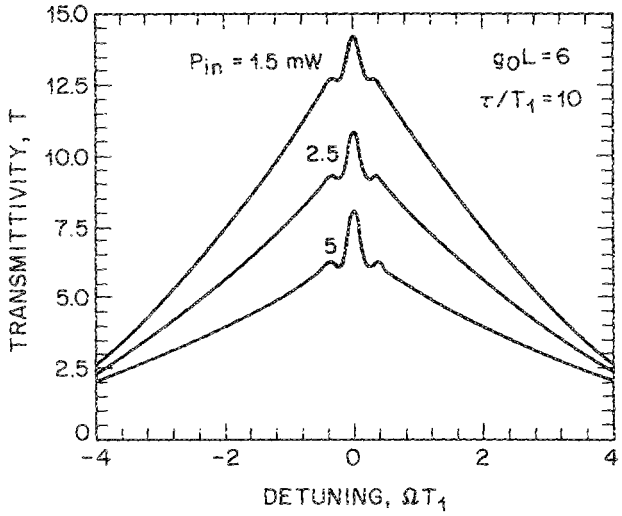

FIG. 2. Variation of the probe transmittivity with the pump-probe detuning ΩT_1 for three values of P_{in}. All parameter values are identical to those of Fig. 1.

Figure 2 shows that the probe transmittivity is also affected by NDFWM, but only in the central region $|\Omega\tau| \lesssim 1$. The main feature is that the transmittivity is considerably enhanced in the presence of NDFWM. This can be understood by noting that the energy conservation requires that for each photon created at the conjugate-wave frequency, a photon is also created at the probe frequency. Thus, the enhancement is due to a transfer of energy from the pump to probe during NDFWM. Clearly NDFWM can considerably affect the gain of a semiconductor-laser amplifier when several beams are simultaneously amplified. This has implications for all-optical fiber-communication systems.

For the case $\beta = 0$ shown in Figs. 1 and 2, the contribution of the index grating to NDFWM has been ignored. When the pump frequency deviates from the gain peak, $\beta \neq 0$ [see Eq. (9)], and the index-grating contribution should be included. For typical parameter values, $|\beta| \sim 0.1$ when the deviation is ~ 1 nm.[10] When $\beta \neq 0$, the probe gain becomes slightly asymmetric with respect to ΩT_1. The effect of index grating on the conjugate reflectivity is almost negligible. This is in contrast to the case considered in Ref. 4, where the dominant contribution to NDFWM comes from the index grating.

In conclusion, an intraband mechanism in semiconductor lasers can lead to significant NDFWM even when the pump and probe frequencies are separated by 100 GHz or more. The physical process is related to spectral hole burning that creates dynamic gain and index gratings at the beat frequency of the pump and probe waves. The efficiency of the gratings is governed by the intraband relaxation time $T_1 (< 1$ ps). This suggests that NDFWM may be useful for estimating T_1 in semiconductor lasers using cw beams, a parameter whose measurement generally requires the use of femtosecond pulses. The NDFWM mechanism considered here may also have applications in high-resolution spectroscopy because of the large range of allowed pump-probe detunings.

[1]For a review, see various articles in *Optical Phase Conjugation*, edited by R. A. Fisher (Academic, New York, 1983).
[2]H. Nakajima and R. Frey, Appl. Phys. Lett. **47**, 769 (1985); IEEE J. Quantum Electron. **QE-22**, 1349 (1986).
[3]R. Frey, Opt. Lett. **11**, 91 (1986); N. C. Kothari and R. Frey, Phys. Rev. A **34**, 2013 (1986).
[4]G. P. Agrawal, Opt. Lett. **12**, 260 (1987).
[5]Y. Nishimura and Y. Nishimura, IEEE J. Quantum Electron. **QE-9**, 1011 (1973).
[6]B. Zee, IEEE J. Quantum Electron. **QE-14**, 727 (1978).
[7]R. F. Kazarinov, C. H. Henry, and R. A. Logan, J. Appl. Phys. **53**, 4631 (1982).
[8]M. Asada and Y. Suematsu, IEEE J. Quantum Electron. **QE-21**, 434 (1985).
[9]R. S. Tucker, J. Lightwave Technol. **LT-3**, 1180 (1985).
[10]G. P. Agrawal, IEEE J. Quantum Electron. **QE-23**, 860 (1987).
[11]G. P. Agrawal and N. K. Dutta, *Long-Wavelength Semiconductor Lasers* (Van Nostrand, Reinhold, New York, 1986), Chap. 2.
[12]T. Fu and M. Sargent, III, Opt. Lett. **4**, 366 (1979).
[13]D. J. Harter and R. W. Boyd, IEEE J. Quantum Electron. **QE-16**, 1126 (1980).